Title
The Northbrae rhyolite of Berkeley (California, USA) constrains motion of the proto-Hayward Fault

Journal
International Geology Review, ahead-of-print(ahead-of-print)

ISSN
0020-6814

Authors
Henschel, Wesley G
Hodgin, Eben B
Grimsich, John L
et al.

Publication Date
2024

DOI
10.1080/00206814.2024.2355620

The Northbrae rhyolite of Berkeley (California, USA) constrains motion of the proto-Hayward Fault

Wesley G. Henschel[1], Eben B. Hodgin[1,2], John L. Grimsich[1], and Nicholas L. Swanson-Hysell[1]

[1] Department of Earth and Planetary Science, University of California, Berkeley, CA, USA

[2] Department of Earth, Environmental and Planetary Sciences, Brown University, Providence, RI 02912

This article was published as:
Henschel, W.G., Hodgin, E.B., Grimsich, J.L., and Swanson-Hysell, N.L. (2024) The Northbrae rhyolite of Berkeley constrains motion of the proto-Hayward Fault, *International Geology Review*, doi:10.1080/00206814.2024.2355620.

Abstract

Right-lateral transform motion associated with the Pacific-North American plate boundary in the modern-day San Francisco Bay Area occurs across a series of sub-parallel fault zones. Much of this motion is accommodated east of the San Andreas fault by the faults of the East Bay fault system. A major tool for reconstructing the spatial and temporal history of fault motion is the correlation of offset Neogene volcanic rocks. These Neogene volcanics within the California Coast Ranges formed in association with the slab gap that grew as the Mendocino Triple Junction migrated northward. Some of the volcanic centers have been variably offset by subsequent strike-slip faulting. A felsic volcanic unit exposed in Berkeley, CA known as the Northbrae rhyolite has variably been interpreted to be one of these Neogene volcanic units or to be a Mesozoic volcanic unit associated with the Coast Range ophiolite. A new U-Pb zircon date of 11.10 ± 0.09 Ma confirms the Neogene volcanic interpretation. This date is indistinguishable from previously published Ar/Ar dates from the Burdell Mountain volcanics of the North Bay region as well as a new U-Pb zircon date of 11.07 ± 0.10 Ma. In addition to the indistinguishable ages, similarities in bulk lithology, zircon crystallization/dissolution textures, and zircon trace element geochemistry are consistent with these rhyolites being associated with the same volcanic center. This correlation implies that 40 ± 5 km of right-lateral offset occurred to the west of the modern-day position of the Hayward-Rodgers Creek fault zone. This offset represents ∼20% of the total offset along the East Bay fault system. A proto-Hayward Fault with a different geometry than that of the present-day played a significant role in the evolution of the fault system. This result highlights the dynamic spatiotemporal variability of strike-slip faults along transform margins.

Introduction

The initiation of the San Andreas Fault system ca. 30 Ma and its subsequent lengthening through to the present-day have led to myriad changes along the California margin (Dickinson, 1981; Powell and Weldon, 1992; Atwater and Stock, 1998). The California Coast Ranges are the expression of this progressive development. The California Coast Ranges are formed of rocks that both pre-date the transform margin as well as sedimentary and volcanic rocks that formed within the transform setting (Fig. 1). The association of volcanism with the transform margin is the result of progressive removal of the previously subducting slab (Fox et al., 1985; Furlong and Schwartz, 2004). Asthenospheric upwelling into the slab gap has resulted in decompression melting and associated volcanism. This upwelling can be imaged in seismic tomography (Liu et al., 2012) and results in anomalous present-day heat flow as well as gravity anomalies to the south of the Juan de Fuca slab edge in northern California (Furlong and Schwartz, 2004). The slab gap mechanism for this California Coast Ranges volcanism was inferred following pioneering efforts to date the volcanic fields (e.g. Turner (1970)). This geochronology revealed an overall trend where most volcanics centers are progressively younger from central California to the northwest towards the Mendocino triple junction (Fox et al., 1985). Comparing geochronology from the volcanic fields with reconstructions of the northward-migrating slab edge reveals an ∼80 km offset between the slab edge and onset of contemporaneous volcanism to the south (Atwater and Stock, 1998; Gerasimov et al., 2024). Given the slab edge's migration rate of 25 km/Myr, this distance corresponds to a time lag of approximately ∼3 Myr between the triple junction's passage and the onset of volcanism at a given location along the margin within the growing slab window.

The northwest age progression of the California Coast Ranges volcanics is complicated by dextral displacements associated with the San Andreas Fault system (Fox et al., 1985; Graymer et al., 2002; Wagner et al., 2011). The fault system varies in complexity along its length from a single strand to more complex configurations such as in the modern-day San Francisco Bay Area where the right-lateral offsets are partitioned across the San Andreas fault, the Hayward-Rodgers Creek faults, the Calaveras fault, and the Greenville fault (Fig. 1; d'Alessio et al., 2005). There has been significant interest in reconstructing the history of how dextral-offsets have been partitioned across these fault systems through time (Wakabayashi, 1999; Graymer et al., 2002; Wagner et al., 2011; Jachens et al., 2017). One tool for such reconstructions has been through the correlation of volcanic centers interpreted to have been originally co-located and subsequently separated through dextral offsets along strike-slip faults (Fox et al., 1985; Graymer et al., 2002; Wagner et al., 2011).

The California Coast Ranges volcanics just north of San Pablo Bay (the northern extension of San Francisco Bay) are a prime example of this dextral strike-slip juxtaposition of volcanic centers of different ages. From west to east, the ca. 11 Ma Burdell Mountain volcanics give way to the ca. 10 Ma Tolay volcanics across the Burdell Mountain and Petaluma Valley faults which give way to the ca. 8 Ma western Sonoma volcanics across the Rodgers Creek fault which in give way to the ca. 5 Ma eastern Sonoma volcanics across the Carneros and West Napa faults (Fig. 1; Wagner et al., 2011). The Tolay volcanics have long been interpreted to be originally contiguous with the Berkeley Hills volcanics (Louderback, 1951; Youngman, 1989). More recent

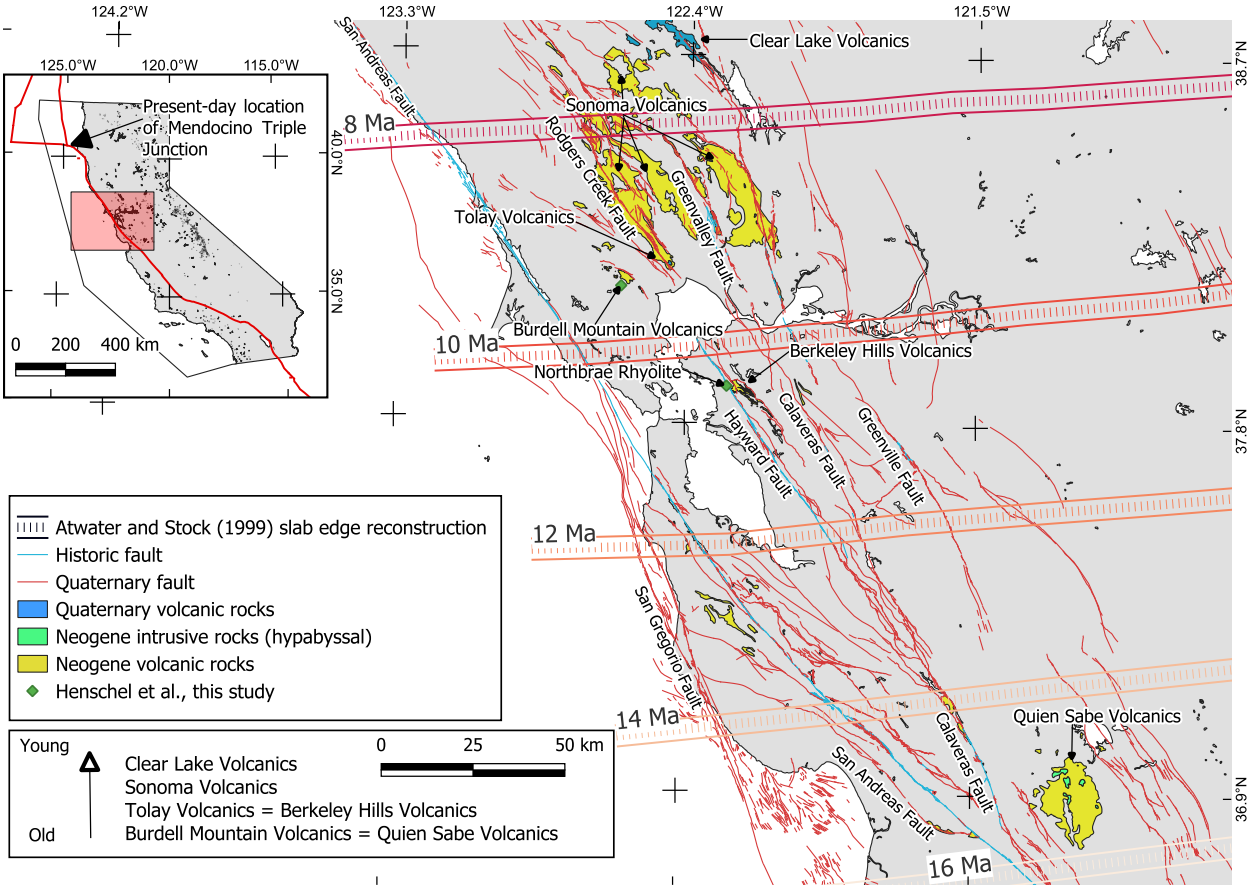

Figure 1. Inset map: An overview map of California, highlighting the Mendocino Triple Junction, the San Andreas fault, and the location of the main map. Main map: Map overview of the San Francisco Bay Area region highlighting Neogene Coast Range Volcanics as well as faults associated with the San Andreas Fault system (Earthquake Hazards Program, 2023). The San Andreas Fault and the faults of the East Bay fault system (e.g. Calaveras and Hayward Faults) diverge in the southernmost portion of the map. The progressive northern migration of the Mendocino Triple Junction is visualized with the Juan de Fuca slab edge reconstruction in two million-year intervals (Atwater and Stock, 1998). Volcanism lagged behind the passage of the slab edge as asthenosphere upwelled into the slab gap. These volcanics are shown following the polygons of Ludington et al. (2005). The locations of studied samples within the Northbrae rhyolite and the Burdell Mountain volcanics are denoted by the green diamonds.

geochronology developed by Wagner et al. (2011) supports the interpretation that the Tolay volcanics were offset by 45 ± 5 km to the NNW relative to the Berkeley Hills volcanics (Graymer et al., 2002). The Burdell Mountain volcanics are interpreted to have originally been associated with the Quien Sabe volcanics to the southeast of San Jose (Fig. 1; Jones and Curtis (1991); McLaughlin et al. (1996); Graymer et al. (2002); Ford (2007)). This interpretation implies that they traveled 175 ± 10 km which has been used as the total offset of the East Bay fault system (i.e. all transform fault motion east of the San Gregorio/San Andreas faults and west of the Central Valley; Graymer et al., 2002). The west-to-east younging of Coast Ranges volcanics across these faults implies progressively less dextral-offset of blocks relative to stable North

America moving east from the Burdell Mountain volcanics (Fig. 1). The 175 ± 10 km estimate of total East Bay fault system offset developed by Graymer et al. (2002) on the basis of volcanic center correlation is similar to the McLaughlin et al. (1996) estimate of 160 to 170 km based on the offset of the Franciscan Complex Permenante Terrane. A similar, albeit larger, estimated offset of 230 to 250 km was developed by Wakabayashi (1999) on the basis of correlations between California Coast Ranges volcanics and Franciscan Complex lithologies.

This contribution is focused on the Northbrae rhyolite of north Berkeley in the eastern San Francisco Bay region. The Northbrae rhyolite is a unit of small areal extent just west of the present-day Hayward Fault (Fig. 1). We are interested in determining whether and how the Northbrae rhyolite fits into this broader context of Coast Ranges volcanism. In particular, we seek to test a hypothesis that the unit is correlative with the Burdell Mountain volcanics, a result which would give significant insight into the partitioning of fault motion along the East Bay fault system over the past 11 million years.

Geologic background

Northbrae rhyolite

The Northbrae rhyolite comprises flow-banded rhyolite which is variably porphyritic, spherulitic, and vesiculated (Palache, 1883; Lawson, 1914). The flow banding has a prominent 1 to 3 cm scale in outcrop along with finer mm-scale laminae (Fig. 2). The flow banding is typically planar with a consistent orientation with locations where it is isoclinally folded. Palache (1883) split the rhyolite into a porphyritic facies, a spherulitic facies, and a glassy facies with the porphyritic and spherulitic facies (which can be gradational between each other) dominating. The porphyritic facies comprises a ground mass of fine intergranular quartz and feldspar with mm-scale phenocrysts of quartz and feldspar. The main mass of Northbrae rhyolite bedrock is a ∼1 x 1.5 km area in northernmost Berkeley, CA with small mapped outliers extending 5 km north into the municipality of El Cerrito (Lawson, 1914; Wakabayashi and Rowe, 2015). The original mapping of Lawson (1914) was before the construction of the current residential neighborhoods which obscure and cover outcrops (with abundant use of the rhyolite within residential retaining walls). Outcrops remain within City of Berkeley parks such as Indian Rock Park (a popular rock climbing locale), Mortar Rock Park, and Great Stoneface Park (Cardwell, 2003).

The Northbrae rhyolite has variably been interpreted as Neogene in age (Lawson, 1914; Radbruch and Case, 1967) or Mesozoic in age (Jones and Curtis, 1991; Graymer et al., 1995). The original Neogene interpretation (specifically Pliocene) of Lawson (1914) was based on the interpretation that the volcanics overlie the Franciscan Complex in angular unconformity. Based on these relationships, Lawson (1914) proposed a Pliocene age, an age that he also assigned to the Berkeley Hills volcanics and terrestrial sedimentary rocks now recognized to be Miocene (Graham et al., 1984; Wagner et al., 2021; Gerasimov et al., 2024). The contact relationships that this assessment is based on are currently obscured, but could have been exposed at the time of Lawson's mapping prior to the construction of the neighborhoods that are now atop of the unit.

An important aspect of the interpretation of the Northbrae rhyolite through the years has been whether or not it is associated with the Leona rhyolite to the south in Oakland (∼5 km south of the Northbrae exposures with outcrops that extend south a further ∼25 km; Robinson, 1953). Lawson (1914) interpreted the Northbrae and Leona units to be distinct. He noted the contrasts between the units with the Northbrae having flow-banding which the Leona lacks and the Leona having abundant sulfides which the Northbrae lacks. Nevertheless, that both are felsic volcanics located in a similar physiogeographic location led to the inference that they are likely the same age (Lawson, 1914; Robinson, 1953). This inference of a similar age led Jones and Curtis (1991) to rule out the Northbrae rhyolite as erupting in the Neogene once they determined the Leona to be Mesozoic in age. Jones and Curtis (1991) wrote: "The siliceous volcanic rocks have long been designated as the Leona Rhyolite and Northbrae Rhyolite of supposed Pleistocene age, but these highly altered rocks are unlike any Neogene volcanic rocks present nearby and are clearly much older ... K-Ar radiometric ages indicate that these rocks are more than 125 Ma old." The K-Ar date referred to in this text is from the Leona rhyolite rather than the Northbrae rhyolite. However, this grouping of the two units into a single mappable unit was formalized with the USGS maps of Graymer et al. (1995) and Graymer (2000). In these maps, the late Jurassic keratophyre and quartz keratophyre unit (Jsv), "includes rocks previously mapped as Leona and Northbrae rhyolite" which Graymer et al. (1995) writes were previously "erroneously considered to be Tertiary (Dibblee, 1980, 1981, Radbruch and Case, 1967, Robinson, 1956)."

An abstract presented at the 2002 GSA Annual Meeting describes research efforts to further study and differentiate the Northbrae and Leona rhyolites (Murphy et al., 2002). In particular, Murphy et al. (2002) states that "zircons collected from the Northbrae gave a tentative Late Miocene age for its formation" (Murphy et al., 2002). These data have never been published although they have been briefly discussed by Wakabayashi and Rowe (2015) who cited Murphy et al. (2002) as demonstrating the error of mapping the Northbrae rhyolite as being Jurassic. Sullivan et al. (2021) cite Murphy et al. (2002) when stating that the age of the Northbrae rhyolite is 11.5 Ma although this specific date is not provided within the cited abstract itself. This same age appears within the Northern California Geological Society field guide of Ford (2003) with references to an undated Murphy personal communication. George Brimhall developed a similar ca. 11 Ma U-Pb zircon date for the Northbrae rhyolite (in a data set that included inherited Mesozoic grains) that he presented in course lectures to students in UC Berkeley's field geology course, but these data were similarly never published. Within the framework of establishing robust piercing points across strands of the East Bay fault system, one goal of our contribution is to clarify the age of the Northbrae rhyolite.

Burdell Mountain volcanics

The unpublished U-Pb zircon dates from the Northbrae rhyolite have led to the inference that it could be correlative to the Burdell Mountain volcanics (Fig. 1; Ford, 2003); although it is an inference that is described by Ford (2003) as being tentative and requiring further research. The Burdell Mountain volcanics include flow-banded porphyritic andesite/dacite/rhyolite as well as volcaniclastic deposits that are exposed immediately west of the Burdell Mountain Fault to the

northwest of San Pablo Bay (Fig. 1; Ford, 2003, 2007; Wagner et al., 2011).

The work of Ford (2007) included four $^{40}Ar/^{39}Ar$ dates for the Burdell Mountain volcanics that were published in Wagner et al. (2011): 11.33 ± 0.07 Ma, 11.12 ± 0.09 Ma, 11.07 ± 0.04 Ma, and 11.02 ± 0.15 Ma. In the context of other dates from Neogene volcanics of the northern San Francisco Bay region, these dates confirmed that the Burdell Mountain volcanics are the oldest. Ford (2007) and Wagner et al. (2011) use the comparison between these dates and published K/Ar dates from the Quien Sabe volcanics ∼175 km to the SSE (Drinkwater et al., 1992) as support of the correlation between the volcanic units. Ford (2007) pointed to similarities in underlying Neogene and Cretaceous sedimentary rocks as well as the metamorphic Franciscan complex as further supporting this correlation.

METHODS and RESULTS

Small fist-sized samples of porphyritic flow-banded rhyolite were collected from the Northbrae rhyolite and Burdell Mountain volcanics for geochronological and geochemical analyses (Fig. 2).

Bulk rock XRF

Two samples from the same rhyolite flow of the Northbrae rhyolite and three samples of rhyolite from the Burdell Mountain volcanics were analyzed for whole rock geochemistry through X-ray fluorescence (XRF). Powders of samples were prepped using an alumina disk within a shatterbox until all powder could be passed through an 80-mesh sieve. At the Franklin and Marshall College X-Ray Laboratory, the powder was pressed into a briquette and then analyzed using a Malvern Panalytical Zetium XRF vacuum spectrometer. These data constrain the samples to be rhyolites with very similar total alkali and silica values (Fig. 3).

U-Pb zircon geochronology

One sample of Northbrae rhyolite (IR22-1) and one of the Burdell Mountain volcanics (BM22-1) were targeted for U-Pb zircon geochronology. Zircon were separated for analysis through standard mineral separation methods at UC Berkeley. Samples were first cleaned with outer regions cut off with a rock saw prior to the pieces being broken down to be run through a disc mill. After being sieved through a 425 μm mesh, zircon were separated with heavy liquids. Zircon were mounted in epoxy, polished to expose their cores, and imaged using cathodoluminescence (CL) and back-scattered electrons on a scanning electron microscope (SEM; Fig. 4). The zircon from both samples are euhedral, prismatic, generally elongate, and rich in melt inclusions (Fig. 4). CL images reveal that zircon from both samples have cores with variable CL zoning often with distinctive CL-dark embayments that can be interpreted to be dissolution-type open-channel melt inclusions (Lerner, 2015). Magmatic zircon overgrowths around the cores typically, but not always, enclose the dissolution-type melt inclusions associated with resorbed cores within the

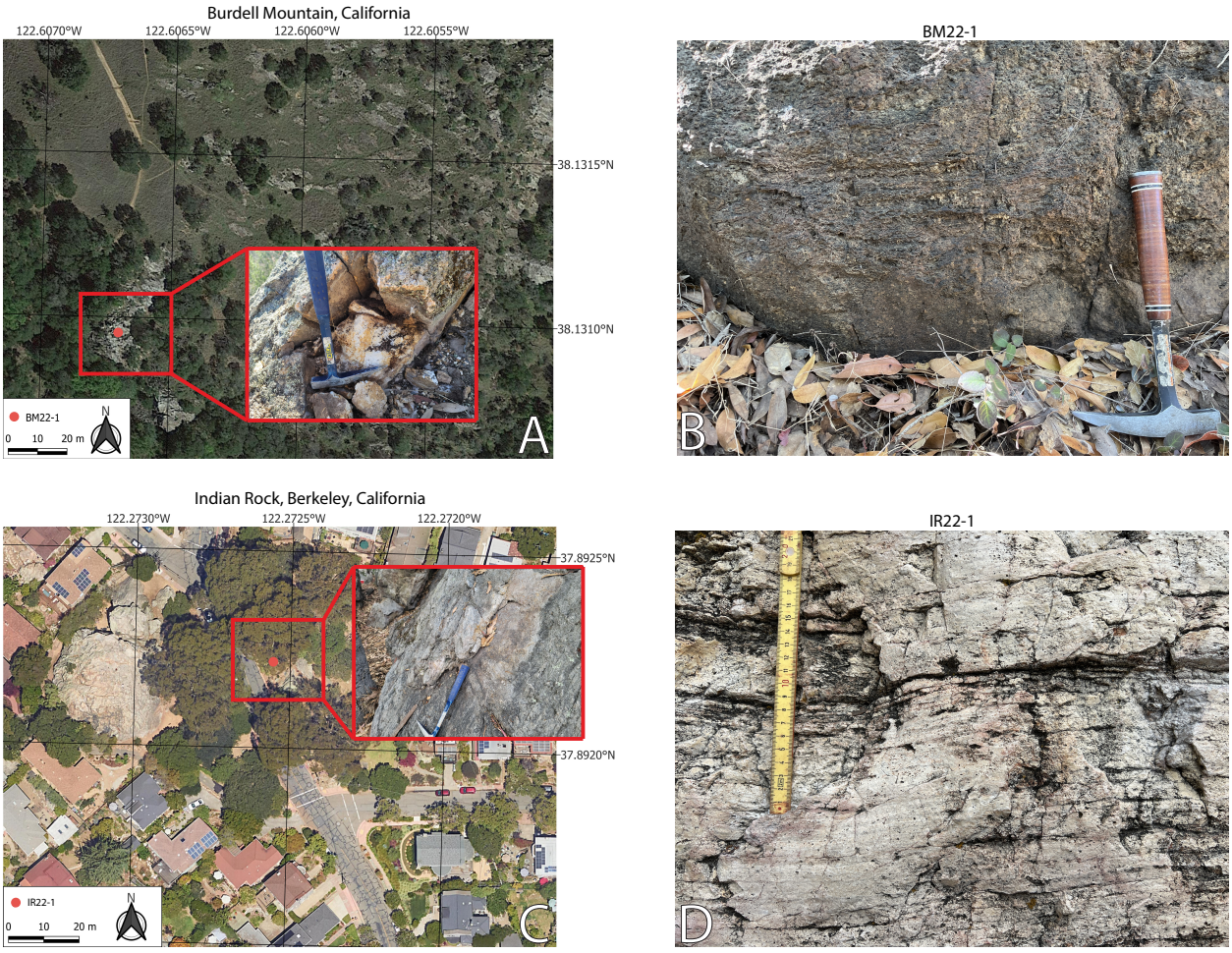

Figure 2. Geographic locations and outcrop photos of Burdell Mountain volcanics sample BM22-1 (A: Sample location 38.130954°N, 122.606703°W. B: Outcrop photo of flow-banding) and the Northbrae rhyolite sample IR22-1 (C: Sample location 37.892218°N, 122.272556°W. D: Outcrop photo of flow-banding). Both samples are from porphyritic flow-banded rhyolites. The maps and sample locations reported use the WGS84 datum.

grain interiors (Fig. 4).

U-Pb ages were obtained through laser ablation inductively coupled plasma mass spectrometry (LA-ICP-MS) at the Boise State University Isotope Geology Laboratory. Laser spot analyses were guided by the CL images. In addition to obtaining ratios for the U-Pb dates, LA-ICP-MS data included trace element geochemistry for the zircon spot analyses. Due to the dissolution-type melt inclusions associated with the embayed zones in some zircon, some analyses had elevated common Pb that were screened from the compiled data (Fig. SI1). This screening was facilitated by the time-resolved signals of the analytes and ratios that are available with the data reduction software. Weighted mean dates from the individual zircon U-Pb dates were calculated using IsoplotR (Vermeesch, 2018).

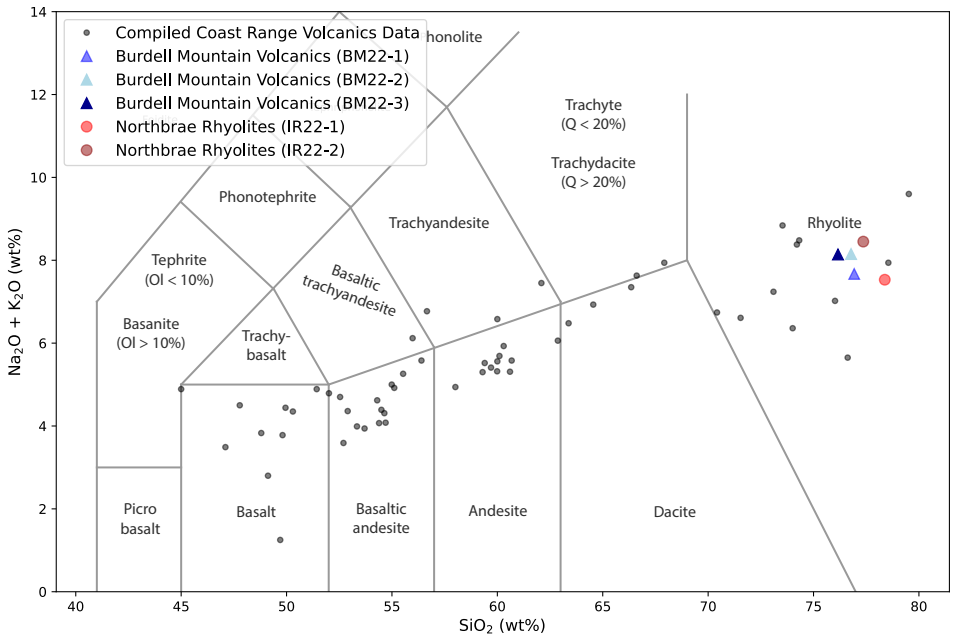

Figure 3. Total alkali-silica (TAS) diagram displaying whole rock geochemical data of the sampled Burdell Mountain volcanics rhyolite and Northbrae rhyolite along with published values from other Coast Ranges volcanics. The Burdell Mountain volcanics and Northbrae rhyolite show striking similarities in SiO_2 and $Na_2O + K_2O$ concentrations compared to previously published Coast Ranges Volcanic data.

Fifty-five LA-ICP-MS analyses were conducted on zircon from the Northbrae rhyolite sample (IR22-1). The detection of common Pb above background levels was the basis for culling 22 analyses. One grain gave a date of ca. 164 Ma and is interpreted as being inherited. The weighted mean U-Pb date of the remaining 34 analyses is 11.10 ± 0.09 Ma with a Mean Square of Weighted Deviates (MSWD) of 1.3 consistent with the grains being from a single population (Fig 5). Zircon core/overgrowth dates from IR22-1 are indistinguishable within analytical precision, indicating that the dated core and overgrowth crystallization events are temporally indistinguishable within error and thus happened in geologically rapid succession (Fig. 4).

Fifty-three LA-ICP-MS analyses were conducted on zircon of the Burdell Mountain volcanics sample (BM22-1). The detection of common Pb above background levels was the basis for culling 14 analyses. Of the remaining 39 analyses, there were four that were assessed to be outliers. The resulting date based on the remaining 35 analyses is 11.07 ± 0.10 Ma with an MSWD of 1.2 (Fig. 5). As with sample IR22-1, the core and overgrowth dates are indistinguishable within uncertainty (Fig. 4). There is a difference in trace elements with the overgrowths having lower Eu/Eu* and lower titanium-in-zircon calculated temperatures of ~690 °C relative to an estimate of ~730 °C for the cores (Figure SI2).

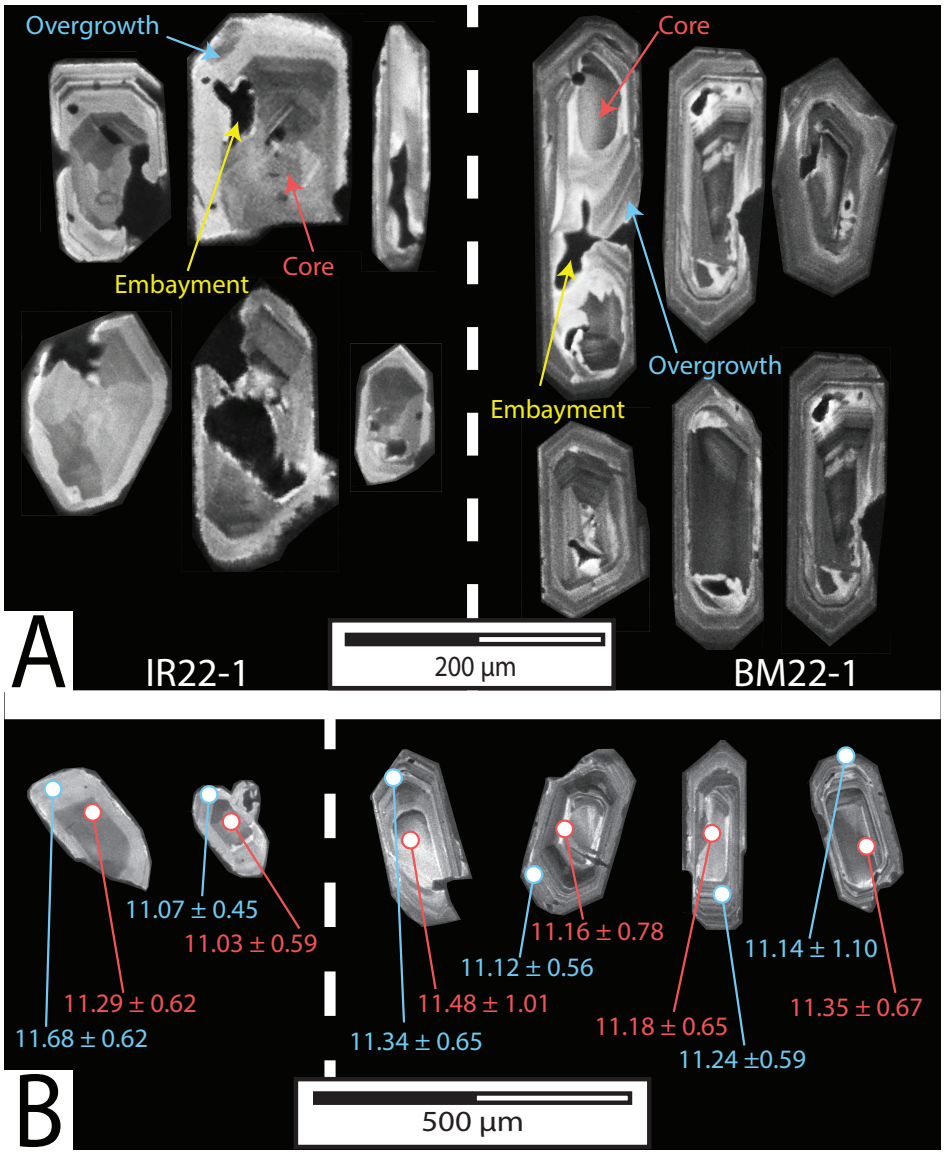

Figure 4. A) Cathodoluminescence (CL) scanning electron microscopy images of Northbrae rhyolite (IR22-1) and Burdell Mountain volcanics (BM22-1) zircon grains exhibiting texturally distinctive embayed and core/overgrowth patterns. The CL-dark embayments are consistent with being dissolution-type open-channel melt inclusions (Lerner, 2015). Example embayed textures are highlighted where irregular CL-dark zones occur within lighter-colored, resorbed zircon domains. The zircon cores and overgrowths are highlighted displaying sector and oscillatory zonation associated with magmatic crystallization. B) CL imagery and LA-ICP-MS U-Pb zircon dates from grains where both cores and overgrowths were dated. The LA-ICP-MS U-Pb zircon dates (with units of Ma) from cores and overgrowths are indistinguishable within analytical precision.

SEM/EDS Analysis

Energy-dispersive X-ray detector (EDS) analysis was conducted using a Zeiss EVO-10 Variable Vacuum SEM at UC Berkeley. Melt inclusions in zircon populations from the Northbrae rhyolite

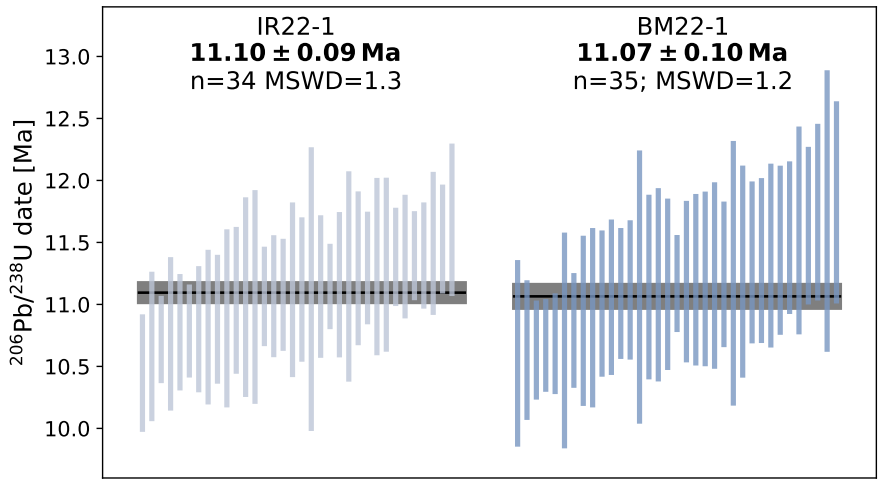

Figure 5. U-Pb date bar plots with individual ^{206}Pb/^{238}U zircon dates and calculated weighted mean dates for samples of the Northbrae rhyolite (IR22-1) and Burdell Mountain volcanics (BM22-1).

(IR22-1) and Burdell Mountain volcanics (BM22-1) were the target of analysis. Melt inclusions were identified from backscatter imagery as darker zones within the light zircon crystals (confirmed to be zircon through their EDS spectra; Fig. SI3). Spots within the melt inclusions were analyzed for ∼45 seconds per location, providing ample time to collect EDS spectra.

EDS spectra analysis of melt inclusions between the two samples showed high concentrations of elements commonly found in alkali feldspars. The inclusions are dominantly cryptocrystalline with no visible crystals in the backscatter imagery (Fig. SI3). EDS spectra of the inclusions are dominated by O, Si, Al, Na, K, and Zr with variable Ca (Fig. SI3). The elemental percentages do not correspond with a distinct feldspar mineral formula, but are characteristic of a silicic alkalic melt. Analyses from both samples exhibit relative similarities between spectra peaks and percent ratios of detected elements. Less commonly, inclusions contain visible oxides in which case there can be Fe and Ti peaks in the spectra. The consistent presence of elevated Zr in the melt inclusions in combination with zircon dissolution texture suggests that the melt inclusions could have incorporated locally-derived zircon melt.

Discussion

Correlation between the Northbrae rhyolite and Burdell Mountain volcanics

The studied rhyolite samples from the Northbrae rhyolite and the Burdell Mountain volcanics both come from flow-banded rhyolite (Fig. 2) with very similar whole rock geochemistry (Fig. 3).

LA-ICP-MS U-Pb dates between the dated Northbrae rhyolite and dated Burdell Mountain volcanics rhyolite are indistinguishable at 11.10 ± 0.09 Ma and 11.07 ± 0.10 Ma respectively (Fig. 5). This result confirms the interpretation of Murphy et al. (2002) that the Northbrae rhyolite is Miocene in age rather than Jurassic. The Northbrae rhyolite is associated with Neogene Coast Ranges slab gap volcanism. While the closest other Neogene volcanics to the Northbrae rhyolite are the Berkeley Hills volcanics on the other side of the Hayward Fault (Fig. 8), those volcanics are younger with the oldest evidence of volcanism being a tuff clast with an a U-Pb zircon date of 10.094 ± 0.018 Ma preserved in a conglomerate just below the in situ volcanics (Gerasimov et al., 2024). The age of the in situ Berkeley Hills volcanics is constrained through a U-Pb zircon date of 9.974 ± 0.014 Ma (Gerasimov et al., 2024) on the Berkeley Hills tuff with sanidine phenocrysts from the same tuff giving an Ar/Ar date of 9.835 ± 0.015 Ma (Fig. 6; Wagner et al., 2021). While the age of the Northbrae rhyolite is distinct from the Berkeley Hills volcanics, the similarity of the Northbrae age with the Burdell Mountain volcanics is consistent with them being associated with the same volcanic center (Fig. 6).

Other lines of evidence associated with both zircon grain morphology and zircon geochemistry further support the Northbrae rhyolite to Burdell Mountain volcanics correlation. In terms of morphology, CL images reveal distinctive textures in zircon from both the Burdell Mountain volcanics rhyolite and Northbrae rhyolite samples (Fig. 4). In both samples, zircon cores are resorbed and can have large CL-dark embayments indicative of dissolution that are typically encapsulated by magmatic zircon overgrowths that grew around the resorbed cores and dissolution-type open-channel melt inclusions (Fig. 4). These textures indicate that after crystallizing from a zircon saturated melt the crystals experienced conditions below zircon saturation that led to dissolution forming the resorbed cores and the channels that filled with melt leading to the inclusions (Fig. 4). When these inclusions were encountered in the LA-ICP-MS analyses they had elevated common Pb values compared to the pure zircon (Fig. SI1), which is consistent with their predominantly feldspathic composition (Fig. SI3). The compositional EDS data from the open-channel melt inclusions is sufficiently similar to the whole rock geochemistry, such that it could be derived from a rhyolitic melt. Zirconium was consistently incorporated into the open-channel melt inclusions, suggesting that zircon dissolution and formation of the open-channel melt inclusions may have happened relatively rapidly before diffusive homogenization with the melt could occur (Nakamura and Shimakita, 1998). The zircon crystals subsequently experienced renewed crystallization associated with zircon saturation prior to eruption leading to the formation of the euhedral and oscillatory-zoned overgrowths. These textures observed for the zircon from both samples are similar to those reported by Lerner (2015) for the Toba eruption, by Wark et al. (2007) for the Bishop Tuff, and by Miller and Wooden (2004) for the Pleistocene Devil's Kitchen rhyolite. In the Devil's Kitchen rhyolite system, the authors favored an interpretation that the dissolution and regrowth of the zircon was the result of the rhyolitic melt being transiently heated through injection of basaltic magma. Heating and subsequent cooling provides a mechanism to alternate from zircon crystallization to dissolution and back to crystallization. For the Devil's Kitchen rhyolite, Miller and Wooden (2004) estimate zircon saturation at a temperature of ∼750 °C. This temperature is similar to that estimated for zircon crystallization using the Ti-in-zircon thermometer (Ferry and Watson, 2007) for both the Burdell Mountain volcanics and Northbrae rhyolite zircon (Fig. 7). Punctuated heating could

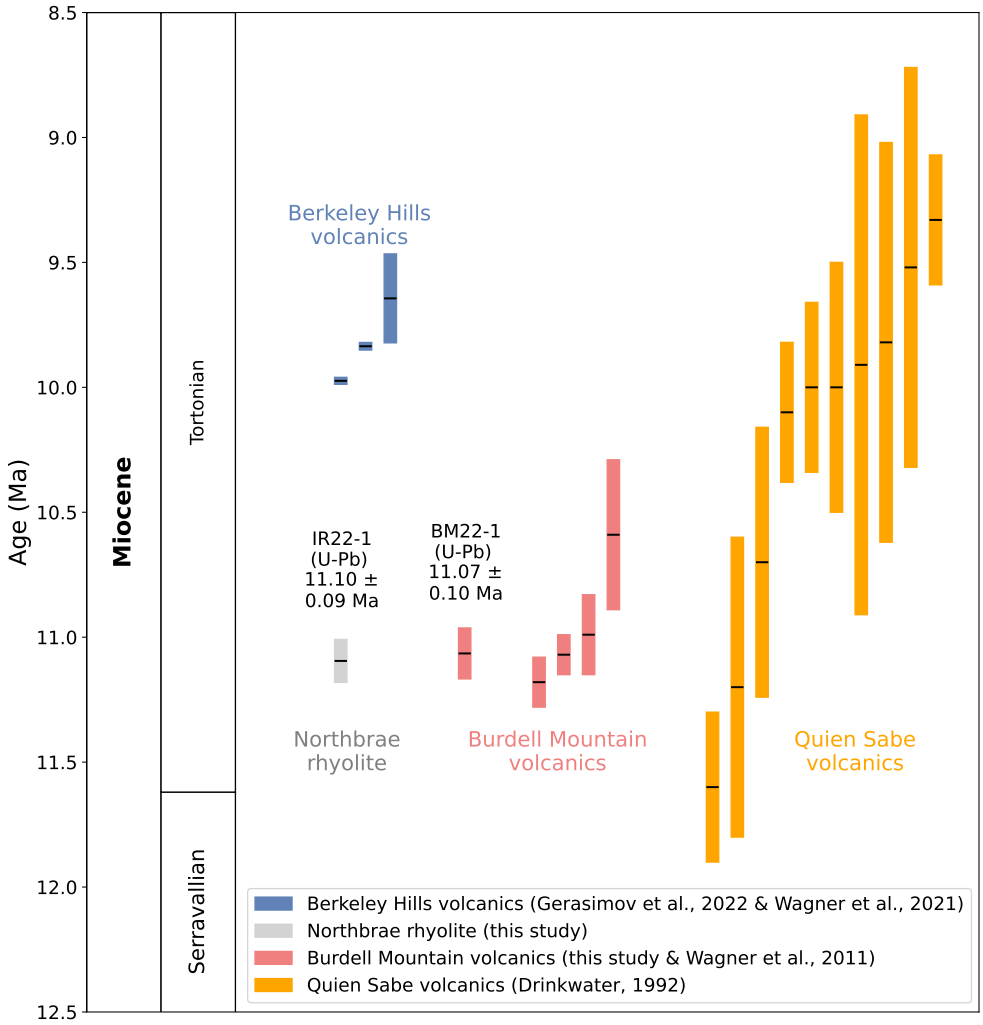

Figure 6. Dates with 2σ uncertainty from California Coast Ranges volcanic centers discussed in the text. The Northbrae rhyolite date (IR22-1) and one of the Burdell Mountain volcanics dates (BM22-1) are from this study, The other Burdell Mountain volcanics dates are $^{40}Ar/^{39}Ar$ dates from Wagner et al. (2011). These dates are similar to the K/Ar dates developed by Drinkwater et al. (1992) from the Quien Sabe volcanics. Dates from the Berkeley Hills volcanics (from Wagner et al. (2021) and Gerasimov et al. (2024)) are younger than those from the Northbrae rhyolite and Burdell Mountain volcanics.

have driven partial zircon dissolution that was followed by a return to zircon saturation through subsequent cooling that resulted in further crystallization. Given that the majority of dissolution-type open-channel melt inclusions have a composition consistent with the rhyolitic composition of the whole rock, the magma recharge event associated with the observed petrogenetic textures need not have been associated with the injection of a mafic melt, but rather could have been driven by injection of felsic melt from within the magmatic system. Our U-Pb data from cores versus overgrowths suggest that the process of core formation, dissolution and open-channel melt inclusion formation, and overgrowth formation occurred rapidly

(indistinguishable within the precision of the LA-ICP-MS analyses) similar to the magmatic timeline from eruptions with petrogenetically similar zircons (Toba Lerner, 2015; Bishop Tuff Wark et al., 2007). That Burdell Mountain volcanics and Northbrae rhyolite samples both show evidence of a similar petrogenetic history recorded by this zircon morphology is intriguing. While this similarity in zircon morphology is not definitive of a correlation in and of itself, it is indicative of similar sequence of pre-eruptive processes occurring in the magmatic system. Combined with the indistinguishable rock types, whole rock geochemistry, and U-Pb dates, the similarity in zircon morphology strengthens the correlation while providing insight into shared magmatic processes.

Further insight can be gained through the chemical composition of the zircon grains. In Figure 7, the rare earth element (REE) distribution profiles are shown for zircon from the Burdell Mountain volcanics and Northbrae rhyolite samples. These REE data are compared to data from zircon from the Berkeley Hills volcanics developed by Gerasimov et al. (2024). The Northbrae and Burdell Mountain zircon have lower heavy REE concentrations than the Berkeley Hills volcanics zircon. Additionally, the Eu anomalies are distinct between the Northbrae/Burdell Mountain zircon relative to the Berkeley Hills volcanics zircon which have lower Eu/Eu* (Fig. 7). The estimated temperatures of crystallization from Ti in the zircon (Ferry and Watson, 2007) are similar but slightly lower in the Berkeley Hills zircon relative to the Northbrae and Burdell Mountain zircon (Fig. 7). The Berkeley Hills volcanics zircon come from dacitic and trachydacite tuffs (Gerasimov et al., 2024) rather than rhyolites which could play a role in these differences. This lithological distinction highlights another difference in that rhyolitic lava flows are not presented within the dominantly basaltic lavas of the Berkeley Hills volcanics.

Overall, the Northbrae rhyolite and the Burdell Mountain volcanics samples have similar bulk lithology, indistinguishable ages, comparable zircon geochemistry, and the same distinctive zircon morphology. Taken together these data support a correlation between the Northbrae rhyolite and the Burdell Mountain volcanics. For each of these data types, the Northbrae rhyolite is more similar with the Burdell Mountain volcanics than with the younger Berkeley Hills volcanics to the east of the Hayward Fault (Fig. 8).

Implications for the East Bay fault system and the temporal evolution of transform margins

The interpreted correlation between the Burdell Mountain volcanics and the Quien Sabe volcanics (Fig. 1) is what constrains the total estimated 175 ± 10 km offset of the East Bay fault system (i.e. all of the faults east of the San Andreas Fault and west of the Central Valley; Graymer et al., 2002). The dates of the Burdell Mountain volcanics, and now the date from the Northbrae rhyolite, overlap with current dates for the oldest Quien Sabe volcanics (Fig. 6); consistent with this widely adopted correlation. However, this assessment is based on low precision K/Ar dates from the Quien Sabe volcanics (Drinkwater et al., 1992). Developing new geochronology data from the Quien Sabe volcanics with modern methods should be a priority for future research in order to more accurately and precisely determine the onset of volcanism.

The correlation of the Northbrae rhyolite with the Burdell Mountain volcanics implies 40 ± 5

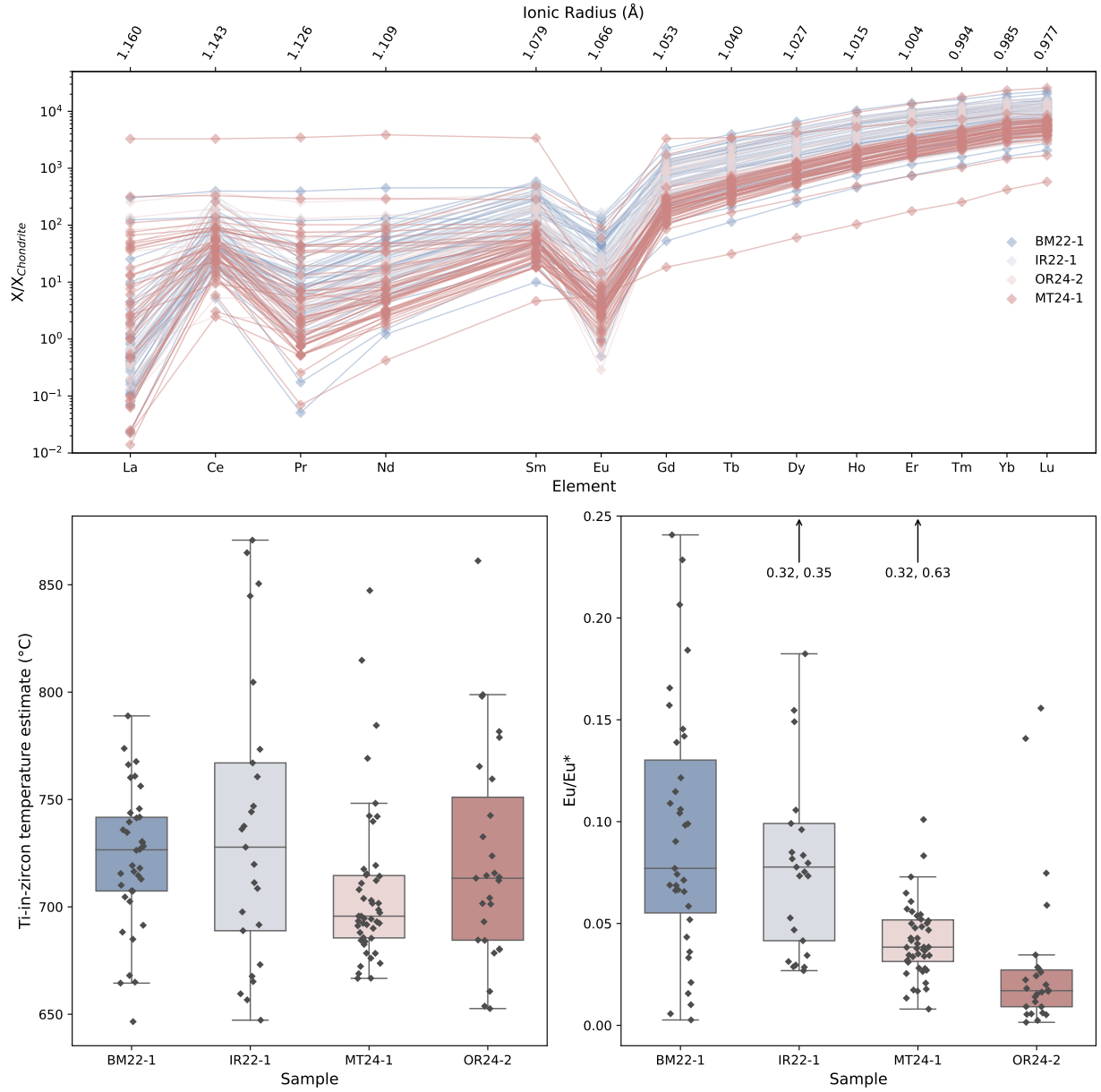

Figure 7. (Top) Rare earth element (REE) profiles between zircon from the Burdell Mountain volcanics (BM22-1), Northbrae rhyolite (IR22-1), and the Berkeley Hills Volcanics (OR24-2 and MT24-1). The REE data are normalized to the chondrite composition model of Palme and O'Neill (2014) as implemented in the Python package pyrolite (Williams et al., 2020). (Bottom Left) Titanium-in-zircon temperature estimates for the BM22-1, IR22-1, OR24-2, and the MT24-1 samples. These values are calculated with an SiO_2 activity of 1.0 given quartz saturation and a constant TiO_2 activity of 0.6 using the calibration of Ferry and Watson (2007). (Bottom Right) Europium anomaly values (Eu/Eu^*) for zircon in the same samples.

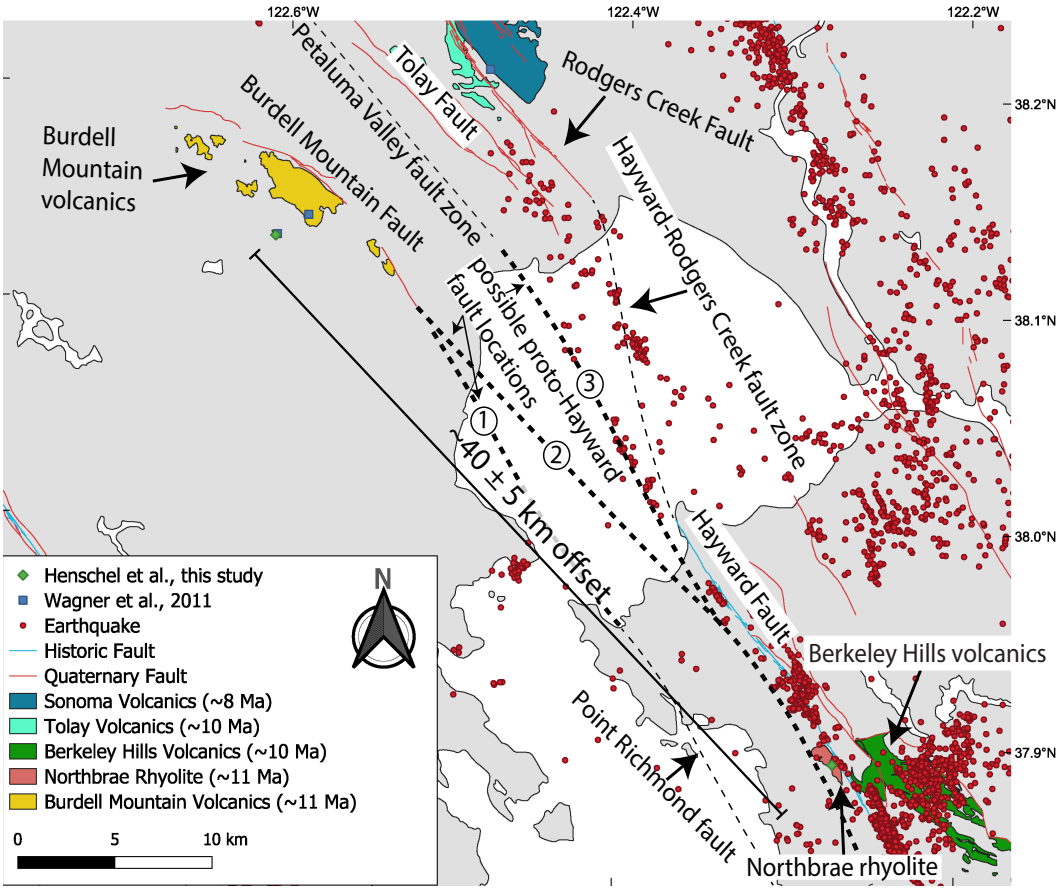

Figure 8. California Coast Ranges volcanic units to the northwest and southeast of San Pablo Bay (the northern portion of San Francisco Bay). Rock units highlighted in this figure show the Northbrae rhyolite (west of the Hayward Fault), Burdell Mountain volcanics, and Berkeley Hills volcanics (east of the Hayward Fault). Bedrock units are adapted from Graymer (2000), Graymer et al. (2006), and Ford (2007). Location of dated samples from this study and Ford (2007); Wagner et al. (2011) are shown. The depicted Quaternary and historic faults are from Earthquake Hazards Program (2023) with the connection between the Hayward and Rodgers Creek Fault as depicted by Watt et al. (2016). The position of the hypothesized Point Richmond fault is shown from Wakabayashi (1999, 2013). The position of the inferred Petaluma Valley fault zone is from Graymer et al. (2002). The correlation between the Northbrae rhyolite and the Burdell Mountain volcanics implies ~40 km of right-lateral offset that would have been accommodated along a strand of the proto-Hayward Fault that could have connected to the Burdell Mountain fault or Petaluma Valley fault. Three possible locations are shown: 1) a connection between the Point Richmond fault with the Burdell Mountain fault; 2) a connection between a fault just west of the Northbrae rhyolite exposures with the Burdell Mountain fault; 3) a connection between a fault just west of the Northbrae rhyolite exposures with the Petaluma Valley fault. Relocated earthquake hypocenters are events between 1984 and 2023 from the Northern California Earthquake Data Center double-difference catalog (Waldhauser and Schaff, 2008; Waldhauser, 2009; Northern California Earthquake Data Center, 2014). Off-fault seismicity to the west of the main Hayward Fault strand could indicate that there is continued reactivation of slip along strands of the proto-Hayward Fault within the modern-day fault zone.

km of dextral offset west of the modern-day Hayward Fault (Langenheim et al. (2010); Fig. 8). In the framework of the interpretation that the Burdell Mountain volcanics were originally colocated with the Quien Sabe volcanics, the Northbrae rhyolite occurs on a fault-bound slice of these volcanics which has been offset from the Burdell Mountain volcanics by fault motion along a proto-Hayward Fault to the west and from the Quien Sabe volcanics by motion along the rest of the East Bay fault system.

Evidence for recent active faulting under San Pablo Bay is interpreted to link the modern-day Hayward Fault to the Rodgers Creek fault with a releasing fault bend geometry (Watt et al., 2016). Such a fault configuration has the potential to explain the offset between the Berkeley Hills volcanics and the correlative Tolay volcanics (Fig. 8). Explaining the offset between the Northbrae rhyolite and the Burdell Mountain volcanics requires offset on a fault strand to the west of the currently active strand of the Hayward Fault. The hypothesized Point Richmond fault of Wakabayashi (1999) to the west of the Hayward Fault is one candidate in this regard (scenario 1 in Fig. 8). For the Northbrae rhyolite and Burdell Mountain volcanics to be offset by a fault in this position, the Northbrae would have needed to extend 5 km west from its current outcrop extent (Fig. 8). It is a hypothesis that is difficult to evaluate given limited exposure but could be consistent with the unit's significant areal distribution (8 km of semi-continuous mapped exposure) along the west side of the Hayward Fault (Lawson, 1914). Relevant to this hypothesis we note that: 1) the same bedrock geology of Franciscan Complex siliciclastics is found beneath the Northbrae volcanics and in exposures just east of the hypothesized Point Richmond fault; and 2) the well-developed dissolution type open-channel melt inclusions in zircons from the Burdell Mountains volcanics and Northbrae Volcanics resemble zircon from very large eruptions with significant areal extent (Lerner, 2015; Wark et al., 2007). If the Burdell Mountain fault links with the Point Richmond fault, then this would suggest that the proto-Hayward could extend as far south as Union City, CA (Wakabayashi, 1999), which is the northernmost extent of the Silver Creek fault (Catchings et al., 2000). The Point Richmond and Silver Creek faults occur in a similar position 5-10 km west of the Hayward Fault, have been inactive for the last 150-200 ka, and each are interpreted to have accommodated ∼40 km of displacement prior to slip migrating farther east (Wakabayashi, 1999; Jachens et al., 2017). If the present-day westward extent of Northbrae rhyolite exposure is close to its original extent, an alternative scenario is one in which there was transform faulting a couple kilometers to the west of the present-day Hayward Fault (scenarios 2 and 3 in Fig. 8). There is seismicity to the west of surface fault creep of the Hayward Fault with this seismicity extending to the western margin of the Northbrae rhyolite (Fig. 8). These earthquakes could potentially be associated with rupture along the western portion of the fault zone that enabled the offset between the Northbrae rhyolite and Burdell Mountain volcanics. Proto-Hayward Fault motion west of the current Hayward Fault (including as far west as the Point Richmond fault) could have connected north to the Burdell Mountain fault or the Petaluma Valley fault as illustrated in Figure 8. Langenheim et al. (2010) highlighted magnetic anomalies aligned between the active trace of the Hayward Fault and these north bay faults near where seismic velocity and gravity gradients are consistent with fault offsets. This overall scenario of the fault history is consistent with the interpretation of McLaughlin et al. (2012) that there was slip on a proto-Hayward Fault system that has appreciable displacement north of Burdell Mountain and to the southwest of the modern-day Rodgers Creek fault zone.

Considering the framework of ∼175 km of total offset on the East Bay fault system, the ∼40 km of offset between the Northbrae rhyolite and Burdell Mountain volcanics is ∼20% of the total motion. This interpretation indicates that ∼20% of the offset along the East Bay fault system occurred west of the modern-day Hayward Fault (Fig. 8).

That this offset implies a proto-Hayward Fault in a different position than its Holocene configuration highlights the spatiotemporal variability of such fault systems. As emphasized in the work of Wakabayashi (1999) and Graymer et al. (2002), transform fault systems are dynamic with time-varying positions of faults and motion along faults. Such time variation has a wide range of implications including the relatively short duration of strike-slip basins (Woodcock, 2004) as zones of transtension can rapidly transition to transpression with changes in fault geometry (Wakabayashi, 2007). Continuing to strengthen correlations between allochthonous blocks of California Coast Ranges volcanics will enable further progress in reconstructing this dynamic tectonic history in space and time.

Acknowledgements

Conversations with Roland Bürgmann gave insight into the active tectonics of the Bay Area. N.L.S.-H. is grateful to George Brimhall for his introduction to East Bay geology and Coast Ranges volcanism in conjunction with passing along the curriculum to the UC Berkeley course EPS 101: Field Geology and Digital Mapping which has been taught continuously since 1890. The manuscript benefited from constructive reviews by Jonathan Miller and two anonymous referees. Research was supported by the UC Berkeley Ramsden Fund for undergraduate research. Mark Schmitz, Jim Crowley, and Darin Schwartz facilitated analyses at the Boise State Isotope Geology laboratory. Stanley Mertzman enabled XRF analyses at Franklin and Marshall College. We thank Yiming Zhang, Shannon Lavelle, and Leah Kahn for their assistance with fieldwork. Data and code for figure generation is available at on Github (`https://github.com/Swanson-Hysell-Group/Northbrae_Volcanics`) and also archived on Zenodo (`https://doi.org/10.5281/zenodo.10611132`).

References

Atwater, T. and Stock, J., 1998, Pacific-North America plate tectonics of the Neogene Southwestern United States: An update: International Geology Review, vol. 40, pp. 375–402, doi:10.1080/00206819809465216.

Cardwell, R., 2003, Northbrae rhyolite field trip: https://www.ncgeolsoc.org/past-field-trips/northbrae-rhyolite-field-trip/, accessed: 2023-10-26.

Catchings, R., Goldman, M., Gandhok, G., Rymer, M., and Underwood, D., 2000, Seismic imaging evidence for faulting across the northwestern projection of the Silver Creek Fault, San Jose, California: Tech. rep., US Geological Survey, doi:10.3133/ofr00125, URL http://dx.doi.org/10.3133/ofr00125.

d'Alessio, M. A., Johanson, I. A., Bürgmann, R., Schmidt, D. A., and Murray, M. H., 2005, Slicing up the San Francisco Bay Area: Block kinematics and fault slip rates from GPS-derived surface velocities: Journal of Geophysical Research, vol. 110, doi:10.1029/2004jb003496.

Dickinson, W. R., 1981, Plate tectonics and the continental margin of California: The geotectonic development of California: Englewood Cliffs, New Jersey, Prentice-Hall, pp. 1–28.

Drinkwater, J., Sorg, D., and Russell, P., 1992, Geologic map showing ages and mineralization of the Quien Sabe Volcanics, Mariposa Peak Quadrangle, west-central California: MF-2200, scale 1:24,000.

Earthquake Hazards Program, 2023, Quaternary fault and fold database of the United States: Tech. rep., USGS, URL https://www.usgs.gov/programs/earthquake-hazards/faults.

Ferry, J. M. and Watson, E. B., 2007, New thermodynamic models and revised calibrations for the Ti-in-zircon and Zr-in-rutile thermometers: Contributions to Mineralogy and Petrology, vol. 154, pp. 429–437, doi:10.1007/s00410-007-0201-0.

Ford, E. W., 2003, Mesozoic and Tertiary stratigraphy of the Burdell Mountain Area and implications for slip along the East Bay Fault System, Marin County, California: Tech. rep., Northern California Geological Society.

Ford, E. W., 2007, Geology of Burdell Mountain and implications for long term slip along the east Bay fault system, California: Master's thesis, San Francisco State University.

Fox, K. F., Fleck, R. J., Curtis, G. H., and Meyer, C. E., 1985, Implications of the northwestwardly younger age of the volcanic rocks of west-central California: Geological Society of America Bulletin, vol. 96, pp. 647–654, doi:10.1130/0016-7606(1985)96⟨647:IOTNYA⟩2.0.CO;2.

Furlong, K. P. and Schwartz, S. Y., 2004, Influence of the Mendocino triple junction on the tectonics of coastal California: Annual Review of Earth and Planetary Sciences, vol. 32, pp. 403–433, doi:10.1146/annurev.earth.32.101802.120252.

Gerasimov, S., Hodgin, E., Crowley, J., and Swanson-Hysell, N., 2024, Chronostratigraphy of Miocene strata in the Berkeley Hills (California Coast Ranges, USA) and the arrival of the San Andreas transform boundary: Geosphere, vol. 20, pp. 162–178, doi:10.1130/GES02650.1.

Graham, S. A., McCloy, C., and Hitzman, M., 1984, Basin evolution during change from convergent to transform continental margin in central California: AAPG Bulletin, vol. 68, doi:10.1306/ad460a03-16f7-11d7-8645000102c1865d.

Graymer, R., 2000, Geologic map and map database of the Oakland metropolitan area, Alameda, Contra Costa, and San Francisco Counties, California: U.S. Geological Survey Miscellaneous Field Studies, vol. MF–2342.

Graymer, R., Moring, B., Saucedo, G., Wentworth, C., Brabb, E., and Knudsen, K., 2006, Geologic map of the San Francisco Bay region, Scientific Investigations Map 2918: Tech. rep., U.S. Geological Survey.

Graymer, R., Sarna-Wojcicki, A., Walker, J., McLaughlin, R., and Fleck, R., 2002, Controls on timing and amount of right-lateral offset on the East Bay fault system, San Francisco Bay region, California: Geological Society of America Bulletin, vol. 114, pp. 1471–1479, doi:10.1130/0016-7606(2002)114⟨1471:COTAAO⟩2.0.CO;2.

Graymer, R. W., Jones, D. L., and Brabb, E. E., 1995, Geologic map of the Hayward fault zone, Contra Costa, Alameda, and Santa Clara Counties, California: A digital database: U. S. Geological Survey Open-File Report 95-597.

Jachens, R., Wentworth, C., Graymer, R., Williams, R., Ponce, D., Mankinen, E., Stephenson, W., and Langenheim, V., 2017, The Evergreen basin and the role of the Silver Creek fault in the San Andreas fault system, San Francisco Bay region, California: Geosphere, vol. 13, pp. 269–286, doi:10.1130/ges01385.1.

Jones, D. L. and Curtis, G. H., 1991, Guide to the geology of the Berkeley Hills, Central Coast ranges, California: *In* Geologic Excursions in Northern California: San Francisco to the Sierra Nevada Special Publication 109, California Department of Conservation, Division of Mines and Geology.

Langenheim, V., Graymer, R., Jachens, R., McLaughlin, R., Wagner, D., and Sweetkind, D., 2010, Geophysical framework of the northern San Francisco Bay region, California: Geosphere, vol. 6, pp. 594–620, doi:10.1130/ges00510.1.

Lawson, A. C., 1914, San Francisco folio, California, Tamalpais, San Francisco, Concord, San Mateo, and Haywards quadrangles: U. S. Geological Survey Geologic Atlas, Folio 193, doi:10.3133/gf193.

Lerner, A., 2015, Insights into the Geochemical Evolution of the Youngest Toba Tuff (Sumatra, Indonesia) Magma Chamber Through the Lens of Zircon-hosted Melt Inclusions: Master's thesis, Oregon State University.

Liu, K., Levander, A., Zhai, Y., Porritt, R. W., and Allen, R. M., 2012, Asthenospheric flow and lithospheric evolution near the Mendocino Triple Junction: Earth and Planetary Science Letters, vol. 323-324, pp. 60–71, doi:10.1016/j.epsl.2012.01.020.

Louderback, G., 1951, Geologic history of san francisco bay: *In* Jenkins, O., ed., Geologic guidebook of the San Francisco Bay counties, California Division of Mines, 154, pp. 75–94.

Ludington, S., Moring, B. C., Miller, R. J., Stone, P. A., Bookstrom, A. A., Bedford, D. R., Evans, J. G., Haxel, G. A., Nutt, C. J., Flyn, K. S., and Hopkins, M. J., 2005, Preliminary integrated geologic map databases for the United States, Western States: California, Nevada, Arizona, Washington, Oregon, Idaho, and Utah: USGS Open-File Report.

McLaughlin, R. J., Sarna-Wojcicki, A. M., Wagner, D. L., Fleck, R. J., Langenheim, V. E., Jachens, R. C., Clahan, K., and Allen, J. R., 2012, Evolution of the Rodgers Creek–Maacama right-lateral fault system and associated basins east of the northward-migrating Mendocino Triple Junction, northern California: Geosphere, vol. 8, pp. 342–373, doi:10.1130/GES00682.1.

McLaughlin, R. J., Sliter, W. V., Sorg, D. H., Russell, P. C., and Sarna-Wojcicki, A. M., 1996, Large-scale right-slip displacement on the East San Francisco Bay Region fault system, California: Implications for location of late Miocene to Pliocene Pacific plate boundary: Tectonics, vol. 15, pp. 1–18, doi:10.1029/95tc02347.

Miller, J. S. and Wooden, J. L., 2004, Residence, resorption and recycling of zircons in Devils Kitchen Rhyolite, Coso Volcanic Field, California: Journal of Petrology, vol. 45, pp. 2155–2170, doi:10.1093/petrology/egh051.

Murphy, L., Fleck, R., and Wooden, J., 2002, Northbrae rhyolite in the Berkeley Hills, CA; A rock well misunderstood: *In* Geological Society of America Abstracts with Programs, vol. 34, p. 363.

Nakamura, M. and Shimakita, S., 1998, Dissolution origin and syn-entrapment compositional change of melt inclusion in plagioclase: Earth and Planetary Science Letters, vol. 161, pp. 119–133, doi:10.1016/s0012-821x(98)00144-7.

Northern California Earthquake Data Center, 2014, NCEDC (2014) Dataset: doi:10.7932/NCEDC, URL `https://doi.org/10.7932/NCEDC`.

Palache, C., 1883, The soda-rhyolite north of Berkeley: University of California Bulletin of the Department of Geology, vol. 1, pp. 61–72.

Palme, H. and O'Neill, H., 2014, Cosmochemical Estimates of Mantle Composition, Elsevier, p. 1â39: doi:10.1016/b978-0-08-095975-7.00201-1.

Powell, R. E. and Weldon, R. J., 1992, Evolution of the San Andreas Fault: Annual Review of Earth and Planetary Sciences, vol. 20, pp. 431–468, doi:10.1146/annurev.ea.20.050192.002243.

Radbruch, D. H. and Case, J. E., 1967, Preliminary geologic map and engineering geologic information, Oakland and vicinity, California, Open-File Report 67-183: Report, USGS, doi:10.3133/ofr67183, URL `https://pubs.usgs.gov/publication/ofr67183`.

Robinson, G. D., 1953, The Leona rhyolite, Alameda County, California: American Mineralogist, vol. 38, pp. 1204–1217.

Sullivan, R., Fay, R. P., Schaefer, C., Deino, A., and Edwards, S. W., 2021, Neogene volcanism on the eastside of Mount Diablo, Contra Costa County, California: *In* Regional Geology of Mount Diablo, California: Its Tectonic Evolution on the North America Plate Boundary, Geological Society of America, pp. 201–228, doi:10.1130/2021.1217(11).

Turner, D. L., 1970, Potassium-Argon Dating of Pacific Coast Miocene foraminiferal stages: *In* Radiometric Dating and Paleontologic Zonation, Geological Society of America Special Paper, pp. 91–130, doi:10.1130/spe124-p91.

Vermeesch, P., 2018, IsoplotR: A free and open toolbox for geochronology: Geoscience Frontiers, vol. 9, pp. 1479–1493, doi:10.1016/j.gsf.2018.04.001.

Wagner, D. L., Saucedo, G. J., Clahan, K. B., Fleck, R. J., Langenheim, V. E., McLaughlin, R. J., Sarna-Wojcicki, A. M., Allen, J. R., and Deino, A. L., 2011, Geology, geochronology, and paleogeography of the southern Sonoma volcanic field and adjacent areas, northern San Francisco Bay region, California: Geosphere, vol. 7, pp. 658–683, doi:10.1130/GES00626.1.

Wagner, J. R., Deino, A., Edwards, S. W., Sarna-Wojcicki, A. M., and Wan, E., 2021, Miocene stratigraphy and structure of the East Bay Hills, California: *In* Regional Geology of Mount Diablo, California: Its Tectonic Evolution on the North America Plate Boundary, Geological Society of America, pp. 331–391, doi:10.1130/2021.1217(15).

Wakabayashi, J., 1999, Distribution of displacement on and evolution of a young transform fault system: The northern San Andreas fault system, California: Tectonics, vol. 18, pp. 1245–1274, doi:10.1029/1999tc900049.

Wakabayashi, J., 2007, Stepovers that migrate with respect to affected deposits: field characteristics and speculation on some details of their evolution: Geological Society, London, Special Publications, vol. 290, p. 169â188, doi:10.1144/sp290.4.

Wakabayashi, J., 2013, Subduction initiation, subduction accretion and nonaccretion, large-scale material movement, and localization of subduction megaslip recorded in Franciscan complex and related rocks, California: *In* Geologic Excursions from Fresno, California, and the Central Valley: A Tour of California's Iconic Geology, Geological Society of America, pp. 129–162, doi:10.1130/2013.0032(07).

Wakabayashi, J. and Rowe, C. D., 2015, Whither the megathrust? localization of large-scale subduction slip along the contact of a mélange: International Geology Review, vol. 57, pp. 854–870, doi:10.1080/00206814.2015.1020453.

Waldhauser, F., 2009, Near-real-time double-difference event location using long-term seismic archives, with application to northern California: Bulletin of the Seismological Society of America, vol. 99, pp. 2736–2748, doi:10.1785/0120080294.

Waldhauser, F. and Schaff, D. P., 2008, Large-scale relocation of two decades of Northern California seismicity using cross-correlation and double-difference methods: Journal of Geophysical Research: Solid Earth, vol. 113, doi:10.1029/2007jb005479.

Wark, D., Hildreth, W., Spear, F., Cherniak, D., and Watson, E., 2007, Pre-eruption recharge of the Bishop magma system: Geology, vol. 35, p. 235, doi:10.1130/g23316a.1.

Watt, J., Ponce, D., Parsons, T., and Hart, P., 2016, Missing link between the Hayward and Rodgers Creek faults: Science Advances, vol. 2, doi:10.1126/sciadv.1601441.

Williams, M., Schoneveld, L., Mao, Y., Klump, J., Gosses, J., Dalton, H., Bath, A., and Barnes, S., 2020, pyrolite: Python for geochemistry: Journal of Open Source Software, vol. 5, p. 2314, doi:10.21105/joss.02314.

Woodcock, N. H., 2004, Life span and fate of basins: Geology, vol. 32, pp. 685–688, doi:10.1130/g20598.1.

Youngman, M. R., 1989, K-Ar and 40Ar/39Ar geochronology, geochemistry, and structural reinterpretation of the Southern Sonoma Volcanic Field, Sonoma County, California: M.s. thesis, University of California, Berkeley.

Supporting Information

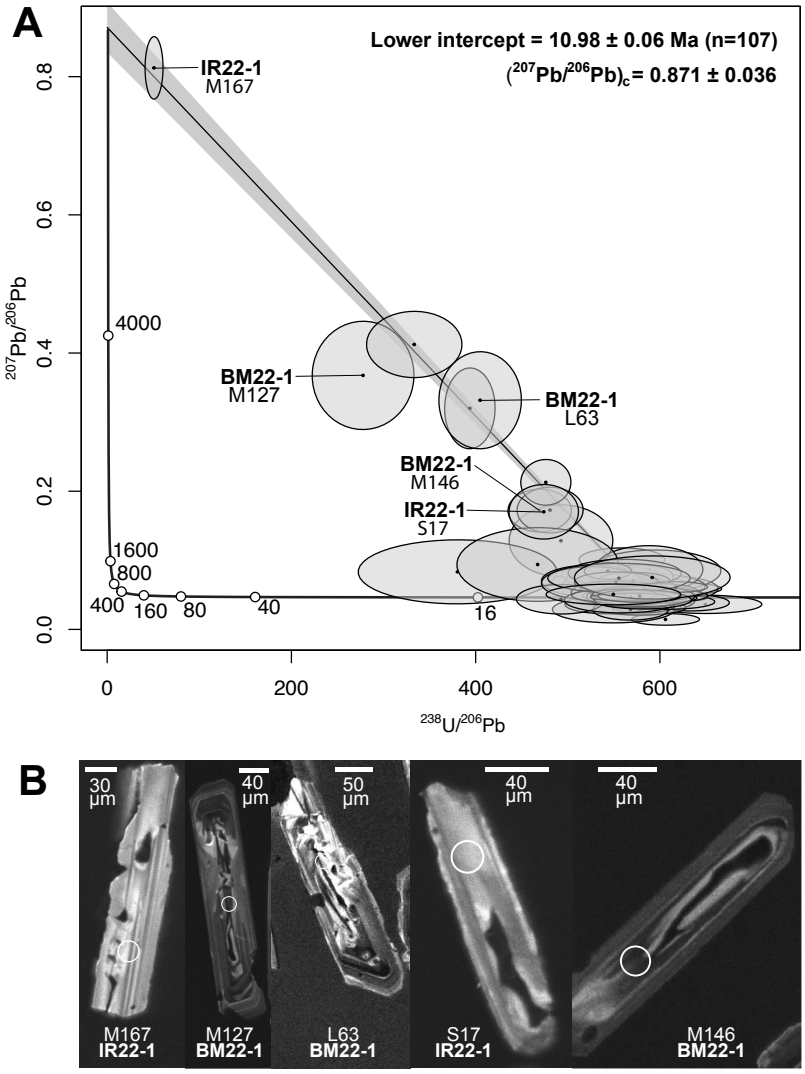

Figure SI1. A) Tera-Wasserburg plot of all unfiltered U-Pb data from BM22-1 and IR22-1 zircon. This plot reveals that there are analyses that have appreciable common Pb (those that are off of the lower intercept). The labeled analyses are shown in the CL imagery in panel (B) and are zircon for which appreciable volume of melt inclusion material was encountered during laser ablation. These melt inclusions can be partially visible at the grain surface. This interpretation that the common Pb incorporation comes from encountering melt inclusions is supported by analytical sweep data monitoring of depth-dependent common Pb counts of the individual analyses. The overlap between BM22-1 and IR22-1 points along the regression line are consistent with a similar $^{207}Pb/^{206}Pb$ composition of the trapped melt between the two samples.

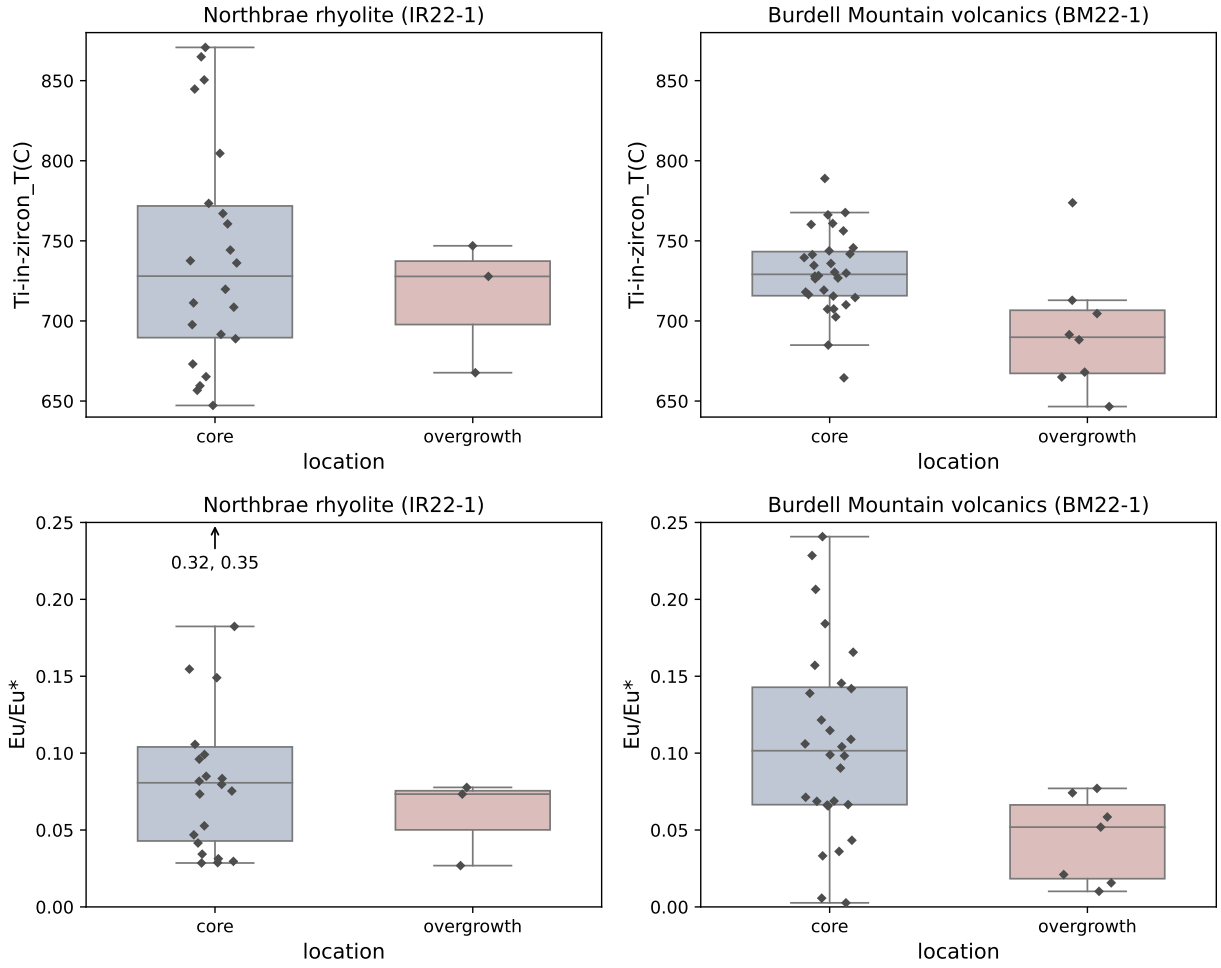

Figure SI2. (Top row) Titanium-in-zircon temperature estimates for zircon from the BM22-1 and IR22-1 samples comparing values from cores vs overgrowths. (Bottom row) Europium anomalies for zircon from the BM22-1 and IR22-1 samples comparing values from cores vs overgrowths.

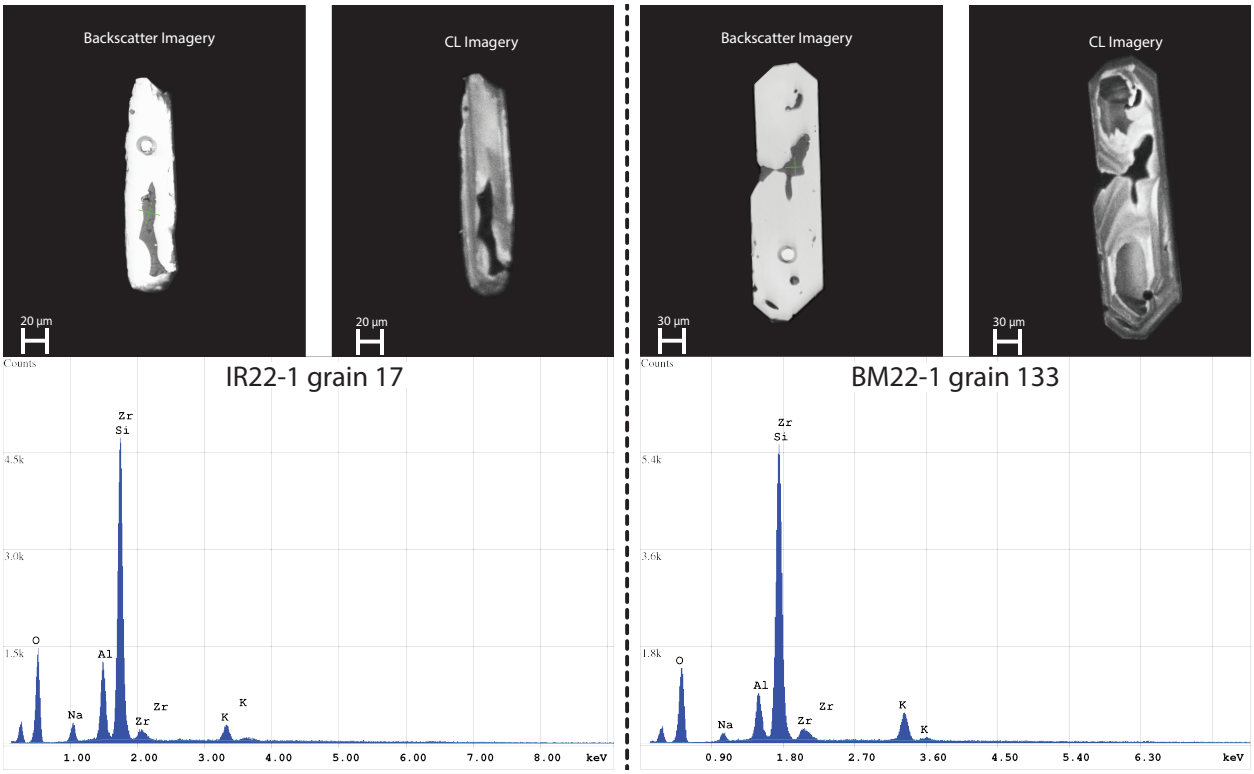

Figure SI3. (Left column) IR22-1 grain number 17 zircon energy dispersive X-ray spectroscopy (EDS) spectra with backscattered electrons (BSE) and cathodoluminescence (CL) images. The EDS spectra was collected at the location of the green cross on the BSE imagery. (Right column) BM22-1 grain number 133 zircon EDS data with associated BSE and CL images.